2015

Effects of CO_2 on Growth Rate, C:N:P, and Fatty Acid Composition of Seven Marine Phytoplankton Species

Andrew L. King

Bethany D. Jenkins
University of Rhode Island, bjenkins@uri.edu

See next page for additional authors

Citation/Publisher Attribution
Andrew L. King, Bethany D. Jenkins, Joselynn R. Wallace, Yuan Liu, Gary H. Wikfors, Lisa M. Milke, Shannon L. Meseck. (2015). "Effects of CO2 on growth rate, C:N:P, and fatty acid composition of seven marine phytoplankton species." *Marine Ecology Progress Series, 537*, 59-69.
Available at: http://dx.doi.org/10.3354/meps11458

Authors
Andrew L. King, Bethany D. Jenkins, Joselynn R. Wallace, Yuan Liu, Gary H. Wikfors, Lisa M. Milke, and Shannon L. Meseck

Vol. 537: 59–69, 2015
doi: 10.3354/meps11458

MARINE ECOLOGY PROGRESS SERIES
Mar Ecol Prog Ser

Published October 14

Effects of CO_2 on growth rate, C:N:P, and fatty acid composition of seven marine phytoplankton species

Andrew L. King[1,2,*], Bethany D. Jenkins[3], Joselynn R. Wallace[3], Yuan Liu[1], Gary H. Wikfors[1], Lisa M. Milke[1], Shannon L. Meseck[1]

[1]Northeast Fisheries Science Center, National Oceanic and Atmospheric Administration, 212 Rogers Ave., Milford, CT 06460, USA
[2]Norwegian Institute for Water Research, Thormøhlensgate 53D, 5010 Bergen, Norway
[3]Department of Cell and Molecular Biology, University of Rhode Island, 120 Flagg Road, Kingston, RI 02881, USA

ABSTRACT: Carbon dioxide (CO_2) is the primary substrate for photosynthesis by the phytoplankton that form the base of the marine food web and mediate biogeochemical cycling of C and nutrient elements. Specific growth rate and elemental composition (C:N:P) were characterized for 7 cosmopolitan coastal and oceanic phytoplankton species (5 diatoms and 2 chlorophytes) using low density, nutrient-replete, semi-continuous culture experiments in which CO_2 was manipulated to 4 levels ranging from post-bloom/glacial maxima (<290 ppm) to geological maxima levels (>2900 ppm). Specific growth rates at high CO_2 were from 19 to 60% higher than in low CO_2 treatments in 4 species and 44% lower in 1 species; there was no significant change in 2 species. Higher CO_2 availability also resulted in elevated C:P and N:P molar ratios in *Thalassiosira pseudonana* (~60 to 90% higher), lower C:P and N:P molar ratios in 3 species (~20 to 50% lower), and no change in 3 species. Carbonate system-driven changes in growth rate did not necessarily result in changes in elemental composition, or vice versa. In a subset of 4 species for which fatty acid composition was examined, elevated CO_2 did not affect the contribution of polyunsaturated fatty acids to total fatty acids significantly. These species show relatively little sensitivity between present day CO_2 and predicted ocean acidification scenarios (year 2100). The results, however, demonstrate that CO_2 availability at environmentally and geologically relevant scales can result in large changes in phytoplankton physiology, with potentially large feedbacks to ocean biogeochemical cycles and ecosystem structure.

KEY WORDS: Phytoplankton · Carbon dioxide · Ocean acidification · Elemental stoichiometry · Fatty acid composition · Diatom · Chlorophyte

INTRODUCTION

The Earth's oceans are an important sink for anthropogenic carbon dioxide (CO_2), being the second largest after the atmosphere (Sabine et al. 2004). The removal of CO_2 from the atmosphere into the world's oceans alters the chemical equilibrium of the seawater carbonate system, resulting in ocean acidification, i.e. a decrease in pH, and an increase in bicarbonate (HCO_3^-) and CO_2. Continuing CO_2 emissions at current rates are predicted to increase the partial pressure of CO_2 (pCO_2) in seawater from the present value of ~400 to ~800–1000 ppm by the year 2100 (IPCC 2007, Tans 2009), resulting in a mean pH drop from 8.2 to 7.8 (Feely et al. 2004). The projected rise in pCO_2 and decline in ocean pH is about 30-fold faster than that observed during the last 300 million years (Kump et al. 2009, Hönisch et al. 2012).

Carbon dioxide and pH play critical roles in mediating physiological functions within marine organisms. Phytoplankton, single-celled photosynthetic organisms that include both calcifying and non-calcifying taxa, play a crucial role in the world's oceans by converting CO_2 to organic C by means of photosynthesis. Laboratory experiments investigating the effects of high CO_2/low pH have revealed potentially

*Corresponding author: andrew.king@gmail.com

Publisher: Inter-Research · www.int-res.com

negative impacts on the physiological and morphological properties of calcifying marine phytoplankton (Riebesell et al. 2000, Orr et al. 2005). The effects of elevated pCO_2 upon phytoplankton also include higher cellular carbon quotas (Burkhardt et al. 1999, Riebesell et al. 2007, Hutchins et al. 2009, King et al. 2011, Reinfelder 2012) and changes in phytoplankton species composition and succession (e.g. Tortell et al. 2002, Riebesell et al. 2013). Higher CO_2 availability could potentially affect phytoplankton community composition by favoring taxa that have less efficient carbon concentrating mechanisms — means of increasing the supply of CO_2, the primary inorganic C source for photosynthesis, to the carboxylating enzyme Rubisco (Roberts et al. 2007b).

Phytoplankton provide organic matter (carbon, nitrogen, phosphorous) and specific nutritional needs (such as polyunsaturated fatty acids) that support the marine food web. For optimal physiological performance of marine metazoans, the trophic transfer, assimilation, and retention of key nutrients contained within phytoplankton is critical. Phytoplankton-produced polyunsaturated fatty acids (PUFA) are considered 'essential' because metazoan organisms require PUFA for growth and are incapable of de novo synthesis (del R. Gonzalez-Baro & Pollero 1988, Kainz et al. 2004). For zooplankton, bivalves, and fish, these fatty acids (FA) are critical for enzyme activity, neural development, stress resistance, membrane fluidity, growth, and survival (Langdon & Waldock 1981, Sargent et al. 1999). Numerous studies have focused on enhanced growth and reproductive rates in the aquatic food web when PUFA and C, N, and P are optimized (Elser et al. 2000, Wacker & von Elert 2001, Sterner & Elser 2002). Slight changes in the nutritional quality of marine phytoplankton (higher C:P or C:N, community FA composition) can result in reduced growth rates and fecundity at higher trophic levels (Sargent et al. 1999). Elevated pCO_2 has been shown to reduce the PUFA content of a cultured diatom (*Thalassiosira pseudonana*) and therefore reduce the PUFA content and hatching success of a copepod grazer reared on the diatom (Rossoll et al. 2012).

Here we present a series of experiments with 7 temperate phytoplankton species, previously isolated from coastal and oceanic locales, grown under carbonate system manipulations that represent the low pCO_2 found in glacial maxima and modern post-bloom scenarios, pCO_2 of present-day average open ocean, pCO_2 predicted by year 2100, and geological maximal pCO_2 levels. The phytoplankton species in this study are relevant in terms of being key species in both the coastal and oceanic marine realms and for use in shellfish aquaculture operations. We show that carbonate system variability can have significant effects upon specific growth rate and elemental stoichiometry on certain species, but this effect differs greatly between species, even between species within the same genus. Despite significant change in growth rate and elemental stoichiometry, there were no significant effects of seawater carbonate manipulation upon FA composition. Findings based upon these phytoplankton species suggest that shifts in CO_2 availability can potentially alter phytoplankton community structure as a consequence of variable growth rate responses, biogeochemical cycling of nutrient elements, and nutritional value in terms of elemental composition, but not PUFA content, of phytoplankton for the marine food web.

MATERIALS AND METHODS

Culture experimental setup

Laboratory cultures were grown aseptically and semi-continuously at 20 ± 2°C under growth-saturating light intensity (~120 µmol photons m^{-2} s^{-1}, 4π detector; 14 h light:10 h dark cycle) in *f*/2 medium made with seawater collected on several occasions from Woods Hole, Massachusetts (Environmental Systems Lab, Woods Hole Oceanographic Institute, MA, USA; salinity = 32–33). After nutrient additions, the culture medium was filter-sterilized (<0.2 µm) into autoclaved 10 l borosilicate glass reservoir containers and adjusted to 4 CO_2 levels by sparging (<100 ml min^{-1}) for a 2 d equilibration period prior to beginning each experiment. After the equilibration period, ~500 to 1000 ml of equilibrated seawater was transferred aseptically into autoclaved, 4 l, borosilicate glass bottles and inoculated with a starter culture (Erlenmeyer flasks with *f*/2 medium) in log growth phase at an initial cell density of $< 5 \times 10^3$ cells ml^{-1}. Each of the 4 CO_2 treatments consisted of 3 replicates (12 experimental bottles total). The same air:CO_2 mixtures were sparged gently into experimental bottles at <30 ml min^{-1}. All air:CO_2 mixtures were filtered with 0.01 µm filter elements (Balston, Parker Hannifin Corp.) prior to entering experimental containers. Growth rates were confirmed to be unaffected by comparing maximum growth rates under unbubbled and bubbled conditions, and to growth rates reported previously in literature. The experimental set up was designed based upon best practice recommendations made by the European Project on Ocean Acidifica-

tion (EPOCA) (Riebesell et al. 2010). A schematic of each experimental unit is shown in Fig. 1.

The 4 CO_2 levels represented a range of physiologically and environmentally relevant levels, consisting of post-bloom/glacial maxima inorganic C availability (less than ~200 ppm pCO_2), present-day open ocean conditions (~350 to 400 ppm pCO_2), future high CO_2/ocean acidification projections (~750 to 1000 ppm pCO_2) (IPCC 2007), and maximum CO_2 availability estimated from the geological record (greater than ~3000 ppm pCO_2) (Kump et al. 2009, Hönisch et al. 2012). Carbon dioxide in the experimental supply air was adjusted using mass flow controllers (Aalborg) that combined air sources of <10 ppm pCO_2 (using a molecular sieve CO_2 adsorber; Puregas) and ~100 000 ppm pCO_2 (AirGas Inc.). For each experiment, each of the 4 target CO_2 levels was achieved by calculating the needed flow rate of each air stream, measuring carbonate system variables, and adjusting flow rate as needed. The pCO_2 in growth media was determined by calculating pCO_2 using CO2SYS (Pierrot et al. 2006), with constants from Mehrbach et al. (1973, refit by Dickson & Millero 1987), and inputs of temperature, salinity, total alkalinity, total dissolved inorganic carbon (DIC), spectrophotometric pH (m-cresol purple), phosphate, and silicic acid. Carbonate system variables from the final time point of each experiment are presented in Table 1. In addition to the endpoint measurement, multiple discrete measurements were made during each experiment to confirm carbonate system manipulations. The standard deviation of pH (total scale) was on average 0.2% (between replicates), the standard deviation of total DIC was on average 0.5% (between replicates), the standard deviation of total alkalinity was on average 0.4% (across all replicates in each of the experiments), and the standard deviation of CO2SYS-calculated pCO_2

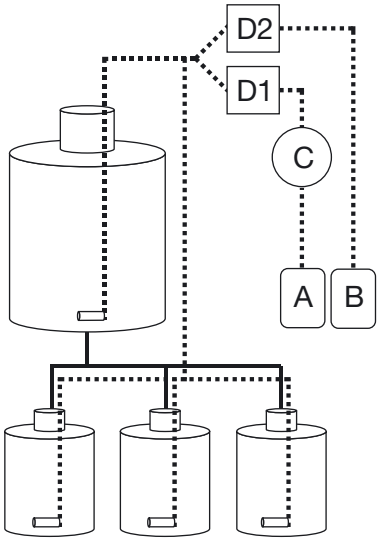

Fig. 1. Schematic of an experimental treatment unit that consists of 1 'reservoir' container (10 l) for dilutions and 3 experimental replicates (4 l). (An experimental system with 4 CO_2 treatments would consist of 4 of these treatment units.) Solid lines refer to tubing for growth medium that are used for making dilutions. Dashed lines refer to gas tubing used for routing different air:CO_2 mixtures to the containers. Labels are as follows: A, compressed air; B, 100 000 ppm CO_2; C, molecular sieve CO_2 adsorber; D1, mass flow controller for low CO_2 air; D2, mass flow controller for 100 000 ppm CO_2

Table 1. Carbonate chemistry at the final time point of experiments listed by species. Average and standard deviation (n = 3) of variables *A* and *B* measured in each experiment are listed (*A* and *B* are denoted as the following: ALK, total alkalinity, µmol kg^{-1}; pH, pH, total scale; DIC, total dissolved inorganic carbon, µmol kg^{-1}). Also included is pCO_2 (ppm) calculated using CO2SYS (see 'Materials and methods')

CO_2 condition (ppm)	*A* Avg.	*A* SD	*B* Avg.	*B* SD	CO2SYS pCO_2 Avg.	CO2SYS pCO_2 SD
Thalassiosira pseudonana **(CCMP1335); *A*: ALK, *B*: pH**						
<230	2282	1	8.602	0.005	73	1
320–390	2304	22	8.064	0.032	381	33
690–1340	2317	14	7.674	0.029	1064	70
2900–5100	2325	7	7.082	0.040	4498	419
Thalassiosira rotula **(GSO101); *A*: DIC, *B*: pH**						
<230	1930	19	8.349	0.004	175	3
320–390	2050	21	8.141	0.027	320	25
690–1340	2222	1	7.863	0.016	689	27
Thalassiosira weissflogii **(CCMP2599); *A*: ALK, *B*: pH**						
<230	2354	11	8.692	0.045	56	8
320–390	2362	15	8.108	0.026	346	28
690–1340	2370	8	7.641	0.014	1183	46
2900–5100	2345	11	7.030	0.010	5111	114
Thalassiosira weissflogii **(CCMP1010); *A*: ALK, *B*: pH**						
<230	2417	10	8.861	0.016	31	2
320–390	2389	10	8.084	0.030	376	31
690–1340	2436	15	7.612	0.031	1316	92
2900–5100	2415	5	7.132	0.011	4157	99
Thalassiosira oceanica **(CCMP1005); *A*: ALK, *B*: DIC**						
<230	2337	7	1798	9	127	2
320–390	2337	3	2020	13	338	21
690–1340	2335	5	2152	3	700	15
2900–5100	2368	9	2384	2	2925	221
Chlorella autotrophica **(CCMP243); *A*: ALK, *B*: pH**						
<230	2318	4	8.253	0.011	223	7
320–390	2298	9	8.058	0.004	386	4
690–1340	2322	1	7.690	0.003	1026	9
2900–5100	2323	6	7.053	0.007	4811	67
Dunaliella salina **(UTEX LB200); *A*: ALK, *B*: pH**						
<230	2362	15	8.549	0.010	91	3
320–390	2388	13	8.115	0.016	343	13
690–1340	2416	9	7.601	0.039	1343	125
2900–5100	2423	47	7.135	0.009	4140	29

was on average <5% (between replicates). The average final time point pCO_2 of each replicate was assigned as the reported pCO_2 value of each experiment (Table 1).

The experiments were conducted with 7 species: coastal diatoms *Thalassiosira pseudonana* (CCMP 1335), *T. rotula* (GSO101; recently deposited as CCMP 3096), and *T. weissflogii* (CCMP2599); oceanic diatoms *T. weissflogii* (CCMP1010 — oceanic isolate) and *T. oceanica* (CCMP1005); and nearshore chlorophytes *Chlorella autotrophica* (CCMP243) and *Dunaliella salina* (UTEX LB200). Cell densities were kept low during the experiments to minimize changes in nutrients and availability of light and dissolved inorganic carbon. Each species was transferred from mid-exponential phase in *f*/2 medium and grown for 7 to 10 generations, after which growth rates stabilized. Cultures were diluted with equilibrated medium every 2 to 3 d, depending upon growth rate. Macronutrients during the experiment always were in excess of 170 µM nitrate, 18 µM phosphate, and 21 µM silicic acid. Cell densities in the experiments were kept low at $<8.5 \times 10^5$ cells ml^{-1} and were on average 3.0×10^5 cells ml^{-1}.

Macronutrient and carbonate system measurements

Nitrate+nitrite, phosphate, and silicic acid were determined using a Quattro autoanalyzer (Seal Analytical). Aliquots of 40 ml were syringe-filtered (0.2 µm), and nutrients were measured within 24 h of collection. All nutrient protocols were developed by the Royal Netherlands Institute for Sea Research. Nitrate+nitrite was determined using the red azo dye method, with a detection limit of 0.02 µmol l^{-1} and a standard deviation of 0.03 µmol l^{-1} (Method NO Q-068-05 Rev. 4). Phosphate was determined using a phosophomolybdenum complex with a detection limit of 0.004 µmol l^{-1} and a standard deviation of 0.01 µmol l^{-1} (Method NO Q-064-05 Rev. 3). A silicomolybdenum blue complex was used to determine silicic acid with a detection limit of 0.05 µmol l^{-1} and a standard deviation of 0.01 µmol l^{-1} (Method NO Q-066-05 Rev. 3).

Sample aliquots for the total alkalinity, total DIC, and pH (total scale) analyses were collected at multiple time points from each experiment to confirm stability of CO_2 manipulations. Total alkalinity was determined using a Gran titration approach with a custom-made, open-cell alkalinity titration system (C. Langdon, University of Miami, FL, USA) equipped with a fine-step, motorized dosing burette coupled with a combination glass/reference pH electrode calibrated against a TRIS HCl buffer (Sigma-Aldrich). The alkalinity titration was performed in a jacketed cell with temperature recorded by an electronic temperature probe (Fisher Scientific Traceable). Total DIC was measured using a DIC analyzer based upon sample acidification and LI-COR CO_2 detection (Apollo SciTech). pH (total scale) was determined colorimetrically using metacresol purple (Sigma-Aldrich) with a Varian dual beam spectrophotometer (Agilent Technologies), 10 cm cylindrical cells (Innovative Lab Supply), and jacketed cell holders, with temperature maintained by a Peltier cooler. The 3 analytical methods in principle are described in detail by DOE (1994). All samples were analyzed within ~5 to 60 min of collection, without the addition of preservatives. Certified reference material for total DIC and total alkalinity was analyzed for accuracy comparisons and, if needed, corrections (A. Dickson, Scrippts Institute of Oceanography/University of California San Diego, CA, USA). In terms of precision, replicate measurements (n = 5) on certified reference material resulted in 1 standard deviation of ±5.5 µmol kg^{-1} for total alkalinity measurements, ±2.7 µmol kg^{-1} for total DIC measurements, and ±0.0014 for total pH. The carbonate system analyses described here were part of an international inter-laboratory comparison exercise that consisted of low and high CO_2 test seawater samples — samples measured using these methods were within 0.5% of assigned values (Bockmon & Dickson 2015).

Physiological measurements

Cell density was measured during the course of each experiment using FACScan and Accuri C6 flow cytometers (Beckton-Dickinson Biosciences). Populations were identified by adjusting voltages and thresholds for forward scatter, side scatter, and chlorophyll auto-fluorescence channels, and collecting data for approximately 1 min. Cell densities were used to make dilution calculations, and specific growth rate calculations were made from the final 3 generations. Particulate organic C, N, and P (POC, PON, and POP, respectively) samples (>200 ml) were vacuum-filtered (<100 mm Hg) onto pre-combusted 24 mm GF/C glass fiber filters (Whatman, GE Healthcare Biosciences) and were determined using conventional methods. Briefly, POC and PON samples were dried in an oven at 60°C, acidified with HCl

fumes, and analyzed using gas chromatography with a CHNSO analyzer (Costech) (Parsons et al. 1984). POP samples were rinsed with 0.17 M Na_2SO_4, dried at 90°C in 0.017 M $MgSO_4$, and measured using the colorimetric molybdate method (Solorzano & Sharp 1980).

FA composition was determined for *T. pseudonana*, *T. weissflogii* (CCMP2599), *C. autotrophica*, and *D. salina*. Sample aliquots (>1.5 l) were vacuum-filtered onto precombusted, 42.5 mm GF/C glassfiber filters, purged with N_2, frozen at −80°C, and subsequently extracted in 2:1 (v/v) chloroform:methanol using a modified Folch procedure (Budge & Parrish 1999). An aliquot of the lipid sample was transmethylated, and fatty acid methyl esters (FAME) were identified on a Shimadzu GC-2014 equipped with an Omegawax 320 column (Supelco). Peak detection used Shimadzu SystemGC software with mixed and individual FAME standards (Supelco, eicosapentaenoic FAME, docosahexaenoic FAME, and PUFA No. III — Menhaden Oil; 47085-U, CRM47571, and CRM47570). Individual FAs and the proportion of total FAs represented by saturated fatty acids (ΣSFA), monounsaturated fatty acids (ΣMUFA), and ΣPUFA were determined by dividing the area of each FAME peak or peak group by the total identified FAME.

RESULTS

Specific growth rates

Over the 4 CO_2 scenarios ranging from <230 to 5100 ppm pCO_2 (Table 1), specific growth rates were found to be significantly different for *Thalassiosira rotula*, *T. weissflogii* (CCMP2599), *T. weissflogii* (CCMP1010), *T. oceanica*, and *Chlorella autotrophica* (1-way ANOVA; $p < 0.05$) (Fig. 2A, Table 2). The *T. rotula* growth rate was 13 and 29% greater at 690 ppm pCO_2, relative to low and present-day pCO_2 levels, respectively. *T. weissflogii* (CCMP2599) and *T. weissflogii* (CCMP1010) growth rates were unchanged between present-day pCO_2 and the geological maxima, but growth rates in the lowest pCO_2 treatment were 60 and 26% lower than growth rates at the geological maxima pCO_2, respectively, for each species (Fig. 2A, Table 2). *T. oceanica* specific growth rates ranged from 19 to 49% lower under high CO_2 conditions (700 and 2925 ppm) relative to growth rates at low pCO_2 and present-day pCO_2 (Fig. 2A). *C. autotrophica* exhibited a significantly higher growth rate at ~1000 ppm pCO_2 — nearly 20% higher than at present-day CO_2 levels (Fig. 2A, Table 2). Specific growth rates for the remaining 2 species, *T. pseudonana* and *Dunaliella salina*, were unchanged across the range of experimental pCO_2 conditions (Fig. 2A, Table 2).

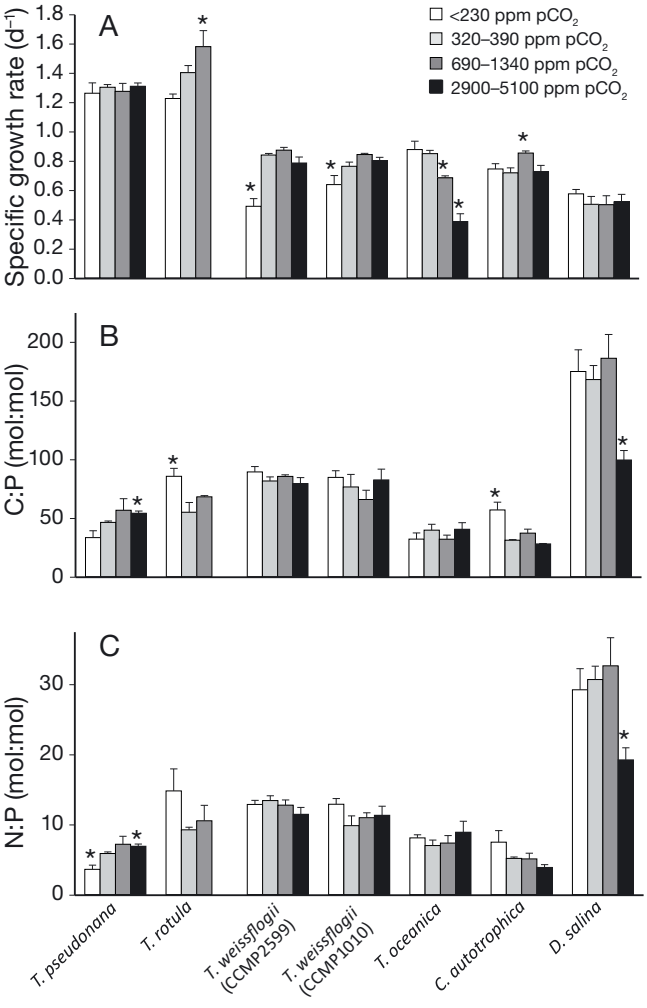

Fig. 2. (A) Specific growth rate (d^{-1}), (B) C:P (mol:mol), and (C) N:P (mol:mol) for 7 phytoplankton species grown under each of the 4 CO_2 conditions, except for *Thalassiosira rotula*, which was grown only under 3 CO_2 conditions. Error bars represent 1 standard error (n = 3). Significant differences relative to present-day pCO_2 are notated with an asterisk (1-way ANOVA; $p < 0.05$). *C.*: *Chlorella*; *D.*: *Dunaliella*

C:N:P composition

Molar ratios of C:P and N:P exhibited some variability between species regardless of CO_2 treatment, with the most notable difference being a several-fold higher C:P and N:P ratio in *D. salina* — ranging from 100 to 186 C:P and 19 to 31 N:P — in comparison with the other 6 species (Fig. 2B). The effects of CO_2 treat-

Table 2. Percent change for significant differences in specific growth rate, μ (d^{-1}), C:P (mol:mol), and N:P (mol:mol) for each of the 7 phytoplankton species (1-way ANOVA; $p < 0.05$). Percent change shown for the highest CO_2 relative to lowest CO_2 treatment (left columns) and for year 2100 CO_2 relative to present-day pCO_2 (right columns). ns: no significant difference (1-way ANOVA; $p > 0.05$)

Species	Highest CO_2 relative to lowest CO_2 treatment (%)			Year 2100 CO_2 relative to present day CO_2 (%)		
	μ	C:P	N:P	μ	C:P	N:P
Thalassiosira pseudonana	ns	62	89	ns	ns	ns
Thalassiosira rotula	29	–20	ns	13	–35	ns
Thalassiosira weissflogii (CCMP2599)	60	ns	ns	ns	ns	ns
Thalassiosira weissflogii (CCMP1010)	26	ns	ns	ns	ns	ns
Thalassiosira oceanica	–44	ns	ns	–19	ns	ns
Chlorella autotrophica	ns	–50	ns	19	ns	ns
Dunaliella salina	ns	–43	–34%	ns	ns	ns

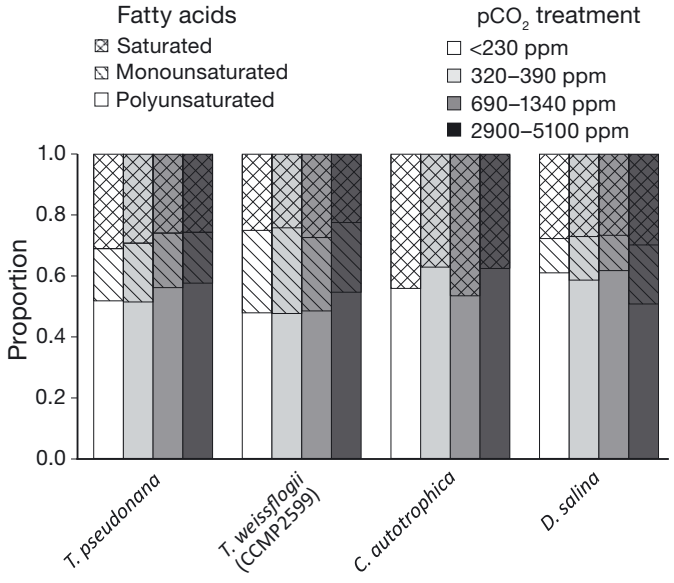

Fig. 3. Fatty acid composition expressed as the contribution of saturated fatty acids (cross-hatched), monounsaturated fatty acids (hatched), and polyunsaturated fatty acids (open) to total fatty acids for *Thalassiosira pseudonana*, *T. weissflogii* (CCMP2559), *Chlorella autotrophica*, and *Dunaliella salina* grown under 4 CO_2 conditions (see gray scale key). Standard errors for fatty acid fractions were on average ±2.1%

ment upon C:P and N:P also varied significantly in 4 of the 7 species (1-way ANOVA; $p < 0.05$) (Fig. 2B,C, Table 2). *T. pseudonana* C:P and N:P were both significantly higher in the geological maxima CO_2 treatment (62% higher C:P and 89% higher N:P in comparison to the lowest CO_2 treatment). In contrast, *T. rotula* and *C. autotrophica* C:P ratios were significantly higher in the lowest pCO_2 treatment (~1.3- to 2.0-fold higher compared to the highest CO_2 treatments, respectively, for each species). C:P and N:P ratios of *D. salina* were not significantly different across the low pCO_2 to year 2100 pCO_2 conditions, but they were 43% (C:P) and 34% (N:P) lower in the highest CO_2 treatment when compared to the lowest CO_2 condition. No significant differences were found in C:P and N:P ratios of *T. weissflogii* (both strains) or *T. oceanica* (Fig. 2B,C).

Fatty acids

There were no detectable differences attributable to pCO_2 treatment in the fractions of total FAs accounted for by ΣPUFA, ΣMUFA, and ΣSFA (1-way ANOVA; $p > 0.05$) (Fig. 3). Additionally, within the ΣPUFA fraction of *T. pseudonana*, *T. weissflogii* (CCMP2599), and *D. salina*, there were no significant differences in the essential omega-3 fatty acids eicosapentaenoic acid (EPA) and docosahexaenoic (DHA). All 3 fractions of FAs were present in *T. pseudonana*, *T. weissflogii* (CCMP2599), and *D. salina*. *C. autotrophica* does not synthesize MUFA or essential omega-3 FAs.

DISCUSSION

The intention of this study was to characterize the responses of individual phytoplankton species grown under various CO_2 conditions, including the ocean acidification (OA) conditions that are projected to occur by the year 2100. To this end, experiments were conducted under nutrient-replete, light-saturating, and controlled and constant inorganic carbonate system conditions. While we acknowledge that carbonate chemistry and multiple other environmental variables in most ocean regimes are dynamic over diel and longer timescales and that these factors certainly affect phytoplankton growth and physiology, characterizing the response of phytoplankton in treatments with constant CO_2/pH and no limitation/co-limitation by other factors is the first step needed in detecting and addressing the potential response of phytoplankton to progressive change in the carbonate chemistry of seawater.

We also acknowledge that geological scale pCO_2 estimates are based on a variety of geochemical proxies (Hönisch et al. 2012) and that evidence sug-

gests that pCO_2 may have co-varied with changes in alkalinity on geological timescales (i.e. elevated pCO_2 in the past may not have resulted in pH declines similar to those projected for the modern OA scenario). Thus, the carbonate system manipulations reported here that consisted of >3000 ppm pCO_2 and modern ocean alkalinity do not necessarily reflect the oceanic carbonate conditions of the geological past, but merely the potential of higher CO_2 availability for phytoplankton that likely evolved under high CO_2 conditions.

Variability in specific growth rates

In the context of phytoplankton community structure and projected success of species under different CO_2 conditions, specific growth rate is a strong determining factor and has therefore been considered a metric of evolutionary fitness (e.g. Collins et al. 2014). There were 4 observed specific growth rate responses to pCO_2 manipulation within the 7 phytoplankton species: no change across all CO_2 treatments (*Thalassiosira pseudonana*, *Dunaliella salina*), higher growth rate at elevated pCO_2 (*T. rotula* and both strains of *T. weissflogii*), lower growth rate at low pCO_2 (*T. oceanica*), and optimal growth rate at an intermediate pCO_2 (*Chlorella autotrophica*) (Fig. 2A). Previously published growth rate responses to CO_2 are in agreement for *T. pseudonana* (no response; Clark & Flynn 2000, Roberts et al. 2007a, Crawfurd et al. 2011, Reinfelder 2012, Yang & Gao 2012, Wynn-Edwards et al. 2014) and *T. weissflogii* (higher growth rate at elevated CO_2; Burkhardt et al. 1999, Shi et al. 2010, Wu et al. 2014). In the case of *T. weissflogii* (CCMP2599 and CCMP1010), specific growth rate is limited only under the lowest CO_2 treatment (<100 ppm pCO_2) and apparently at maximal present-day pCO_2 (~350 to 380 ppm) and at pCO_2 representative of future projections and the geological past.

The positive response of *T. rotula* and *C. autotrophica* specific growth rates to high CO_2 availability in OA scenarios suggests that these 2 species could benefit from the projected increase in oceanic pCO_2 within the next century. Although elevated CO_2 conditions would provide an evolutionary advantage if competition were dictated purely by CO_2 availability, it remains unclear how this response would play out under natural conditions in which these species may respond differently to multiple environmental variables (e.g. temperature, light, and nutrient availability), in addition to ecological interactions including grazing and allelopathy. Indeed, a number of natural community CO_2 manipulation experiments ranging from liters to 1000s of liters in scale have shown a variety of different responses in terms of phytoplankton community structure (Tortell et al. 2002, Feng et al. 2009, Riebesell et al. 2013).

The growth rate responses among the 7 species also provide clues as to the degree to which each species could have been carbon limited prior to the industrial revolution. The slower growth rates of *T. rotula* and *T. weissflogii* (both strains) under the low CO_2 treatment indicate that these species could have been limited by low CO_2 availability in the past, while the growth rates of *T. pseudonana*, *T. oceanica*, and both chlorophytes appear to be unaffected by low CO_2 availability. A possible explanation could be that the latter species possess carbon concentrating mechanisms that are active and/or efficient enough to supply adequate CO_2 to the chloroplast. Another possible mechanism that could explain possible C limitation is cell size and the resulting limitation of CO_2 diffusion and/or the density of inorganic C transporters on the cell surface arising from the low ratio of surface area: volume (Finkel et al. 2010, Wu et al. 2014). *T. rotula* and *T. weissflogii* (both strains) both had enhanced growth rates at higher pCO_2, and are relatively large diatoms with maximal cell lengths ranging from ~18 to 60 µm. While *T. pseudonana* (no growth response) and *T. oceanica* (negative growth response) are morphologically similar to *T. rotula* and *T. weissflogii*, their maximal cell lengths range between ~5 and 12 µm. Neither *C. autotrophica* nor *D. salina* growth rates exhibited apparent limitation by C availability, and both are also relatively small with maximal cell lengths ranging from ~5 to 15 µm.

The negative growth rate response of *T. oceanica*'s to high CO_2/low pH conditions was not observed in any of the other species in the present study. Shi et al. (2010) observed a positive response of *T. oceanica* growth rate to pCO_2 enrichment ranging from ~100 to 680 ppm pCO_2 (same strain used in the present study; CCMP1010). Some diatoms, however, in other studies (*Phaeodactylum tricornutum*, *T. pseudonana* [also CCMP1335], and *Skeletonema costatum*) have been reported to exhibit between ~10 and 16% lower growth rates when grown under high CO_2 conditions (~1000 ppm pCO_2) in combination with high light intensities (>200 µmol photons m^{-2} s^{-1}) (Gao et al. 2012). Hypothetically, a lower growth rate under high light intensities and elevated carbon availability could be a result of reduced energy requirements for inorganic C acquisition combined with the lack of alternate energy-shunting mechanisms (Gao et al. 2012) or the downregulation of carbon concentrating mechanisms

and reduction in inorganic carbon availability, resulting in a reduction in photosynthetic saturation irradiance (Hoppe et al. 2015). Although the experimental light intensity used in the present study was well below 200 µmol photons m^{-2} s^{-1}, reduced growth rates could potentially be a manifestation of the interactive effects of reduced energy requirements for carbon-concentrating mechanisms under high CO_2/low pH and the cell's inability to cope with excess light (i.e. lack of photoprotective mechanisms) (Wu et al. 2010). Indeed, *T. oceanica* has been shown to perform well at light intensities that are lower relative to those of neritic species (e.g. Sakshaug et al. 1987).

In addition to the potential light–CO_2 interaction, *T. oceanica* and other oceanic isolates might be less likely to experience large diel/seasonal fluctuations in comparison to coastal isolates, whereby pCO_2 could be more variable due to coastal upwelling of high pCO_2 waters and low pCO_2 post-bloom periods. While *T. oceanica* growth rates did show sensitivity to elevated pCO2, the growth rate response of *T. weissflogii* (CCMP1010 — oceanic isolate) was not different than that of the coastal isolate of *T. weissflogii* (CCMP2599) (Fig. 2).

Elemental composition

Elemental composition of each of the 7 species can be compared with the molar ratios reported for a number of species from similar genera grown under uncontrolled CO_2 conditions in the artificial seawater medium Aquil (Quigg et al. 2003). The molar ratios of C:P of ~200 and N:P of ~30 that were observed for *D. salina* were similar to those observed for *D. tertiolecta*, and the C:P molar ratios <100 and N:P <15 were also observed in diatoms, including a diatom from the genus *Thalassiosira* (Quigg et al. 2003) (Fig. 2B,C). Similar to the growth rate response to varying CO_2 levels, several response patterns were evident in C:P and N:P molar ratios of the 7 species: no statistical difference across all 4 CO_2 treatments (*T. weissflogii* CCMP2599, *T. oceanica*), higher C:P and N:P molar ratios under high CO_2 conditions (*T. pseudonana*), and higher molar ratios under low CO_2 conditions (*T. rotula*, *C. autotrophica*, and *D. salina*) (Fig. 2B,C; Table 2). The positive relationships between C:P and N:P molar ratios and CO_2 for *T. pseudonana* are consistent with previously published results from other studies involving *T. pseudonana* (Reinfelder 2012) and various other diatoms (Burkhardt et al. 1999, King et al. 2011). Significantly higher C:P under low CO_2 observed in *T. rotula* is consistent with C:P molar ratios reported for *T. weissflogii* (unknown strain) (Burkhardt et al. 1999). With regards to the OA scenarios expected within the next century, we did not detect any significant differences in C:P and N:P molar ratios between present-day pCO_2 and elevated pCO_2 treatments.

Consistent with previous work, the present study suggests that phytoplankton have nutrient requirements that are quite plastic (even within the same genus, as is shown here for *Thalassiosira*). For instance, changes in growth rate (and CO_2 availability) can occur with no change in elemental stoichiometry (both strains of *T. weissflogii* and *T. oceanica*), or no change in growth rate can occur with significant differences in elemental stoichiometry (*T. pseudonana*, *D. salina*). Knowing that C, N, and P are required for basic cell functions associated with growth (proteins, amino acids, RNA, phospholipids, etc.) and that bulk measurements constitute an integration of a multitude of cell functions, it remains a challenge to predict how elemental requirements (either absolute or as ratios) might change in response to growth rate and/or CO_2 availability (Burkhardt et al. 1999, Reinfelder 2012).

The plasticity and variability in elemental stoichiometry shown here for these 7 phytoplankton species are relevant for marine ecosystem structure in 2 respects. First, phytoplankton elemental stoichiometry combined with growth rate, to a large extent, influences nutrient cycling through uptake in the euphotic zone and the distribution of nutrients in the deep ocean through export and subsequent remineralization. Phytoplankton elemental stoichiometry, especially N:P molar ratios, can also influence temporal patterns in phytoplankton community structure in relation to the potential limitation/co-limitation associated with nitrate and phosphate availability — 2 elements that often are limiting in marine systems. Second, phytoplankton with higher C:P molar ratios have been shown to be lower in nutritional quality for grazers because C tends to be in excess relative to growth-limiting P (Elser et al. 2000, Urabe et al. 2003, Schoo et al. 2013). It is hypothesized that the effort involved in respiring food sources with excess C reduces the potential for somatic growth, and the decline in phytoplankton C:P molar ratios within the last ~500 million years, largely associated with the proliferation of diatom and dinoflagellate lineages, has been linked to the rise of modern metazoans (Martin et al. 2008). The influence of CO_2 upon phytoplankton elemental stoichiometry must also be considered in concert with other environmental factors such as nutrient and light availability which can likewise affect stoichiometry significantly (Finkel et al. 2010).

Fatty acid composition

In the present study, we did not detect significant CO_2/pH-driven effects upon the fraction of total FAs accounted for by ΣPUFA in 2 diatom species or in 2 chlorophyte species, nor did we detect a significant omega-3 FA contribution to total FAs in the 2 diatoms (Fig. 3). No change in PUFA content at elevated pCO_2 (~960 to 1000 ppm) was found for the Antarctic prymnesiophyte *Phaeocystis antarctica*, the dinoflagellate *Gymnodinium* sp. (Wynn-Edwards et al. 2014), or for the sea-ice diatom *Nitzschia lecointei* grown at 2.5°C (this was not true at −1.5°C) (Torstensson et al. 2013). A recent study with *T. pseudonana*, however, reported a ~38% decline in total FAs cell^{-1} at 915 ppm pCO_2 relative to 365 ppm pCO_2, and a ~20% decline in the PUFA fraction of total FAs (Rossoll et al. 2012). Similar trends in declining PUFA content at elevated pCO_2 were reported for the Antarctic prasinophyte *Pyramimonas gelidicola* (Wynn-Edwards et al. 2014), the sea-ice diatom *N. lecointei* when grown at −1.5°C (but not at 2.5°C) (Torstensson et al. 2013), and the diatom *Cylindrotheca fusiformis* (Bermúdez et al. 2015). In a mesocosm CO_2 experiment with natural phytoplankton assemblages, PUFA were found to increase under high CO_2 primarily, but this was identified to likely be caused by a shift in community structure from diatoms to dinoflagellates, the latter of which had a relatively higher PUFA content (Leu et al. 2013). Although the mechanisms behind CO_2/pH-driven effects upon phytoplankton FA composition remain elusive, there does appear to be a relationship between low pH, reduced FA synthesis, and FA desaturation (Sato et al. 2003), in addition to a temperature–CO_2/pH relationship and the degree of saturation in proposed interactions between membrane fluidity, temperature, and maintenance of internal pH (Teoh et al. 2004, Mayzaud et al. 2013, Torstensson et al. 2013). Growth phase (logarithmic or stationary) is often difficult to control in dense cultures and is likely a confounding factor in findings to date.

CONCLUSIONS

In a series of culture experiments with controlled carbonate chemistry and nutrient-replete and light-saturating conditions, we have shown that the response of growth rate and elemental composition of 7 phytoplankton species (5 diatoms and 2 chlorophytes) to CO_2/pH differs between species. For a subset of these species in which FA composition was examined, there were no detectable effects of elevated CO_2 upon FA composition, including the fraction of FAs accounted for by PUFA. In terms of OA scenarios projected for the next century, significant findings are limited to increased growth rate of *T. rotula* and *C. autotrophica*, and decreased growth rate of *T. oceanica*. A number of other growth rate and elemental stoichiometry effects were found for other species under very low (<215 ppm pCO_2) and very high (>2900 ppm pCO_2) CO_2 conditions. The responses found in these CO_2 treatments are of potential utility when examining phytoplankton biogeochemical processes during transient post-bloom conditions in modern oceans, as well as over geological timescales.

Characterizing the effects of CO_2 availability upon phytoplankton growth and physiology is crucial for several scientific needs: (1) improving our understanding of variability in oceanic primary production on numerous spatial and temporal scales, (2) understanding potential effects of this variability upon global and ocean nutrient cycles, and (3) determining resources available to higher trophic levels that depend upon phytoplankton for nutrition. Notably, CO_2-driven changes in growth rate were not necessarily reflected in significant changes in elemental composition or FA composition, and vice versa. This is exemplified by the nearly 2-fold range of plasticity that was found in C:P and N:P molar ratios, despite a relatively unchanged specific growth rate. Generalizations regarding the effects of variable CO_2 availability upon phytoplankton in general are difficult to make because of the observed occurrence of both bidirectional (or perceived positive or negative) responses to changes in CO_2. Predictions of future ocean biogeochemical and ecosystem structure responses to the oceanic uptake of anthropogenic CO_2 are dependent upon characterizing the response and sensitivity of phytoplankton to elevated CO_2 (and other environmental factors). This clearly requires further work towards identifying and understanding the mechanism(s) responsible for change and towards parameterizing and constraining oceanic biogeochemical models.

Acknowledgements. We thank M. Dixon, J. Alix, S. Pitchford, D. Kapareiko, K. Hamel, K. Boeff, K. Dickinson, Z. Cao, B. Alix, and G. Bernatchez for technical assistance; D. McCorkle and R. Belastock for facilitating access to the WHOI ESL seawater pumping system; J. Wells (Memorial University Newfoundland) for technical assistance with fatty acid methyl ester analyses; and 3 anonymous reviewers for comments that improved the manuscript. Funding was provided by the NOAA Ocean Acidification Program (OAPFY11.01, FY12.02,

FY13.03.NEFSC.001), the National Science Foundation to B.D.J. (OCE0962208), and the National Research Council Research Associateship Program (A.L.K.).

LITERATURE CITED

Bermúdez R, Feng Y, Roleda MY, Tatters AO and others (2015) Long-term conditioning to elevated pCO_2 and warming influences the fatty and amino acid composition of the diatom *Cylindrotheca fusiformis*. PLoS ONE 10:e0123945

Bockmon EE, Dickson AG (2015) An inter-laboratory comparison assessing the quality of seawater carbon dioxide measurements. Mar Chem 171:36–43

Budge SM, Parrish CC (1999) Lipid class and fatty acid composition of *Pseudo-nitzschia multiseries* and *Pseudo-nitzschia pungens* and effects of lipolytic enzyme deactivation. Phytochemistry 52:561–566

Burkhardt S, Zondervan I, Riebesell U (1999) Effect of CO_2 concentration on C:N:P ratio in marine phytoplankton: a species comparison. Limnol Oceanogr 44:683–690

Clark DR, Flynn KJ (2000) The relationship between the dissolved inorganic carbon concentration and growth rate in marine phytoplankton. Proc R Soc B 267:953–959

Collins S, Rost B, Rynearson TA (2014) Evolutionary potential of marine phytoplankton under ocean acidification. Evol Appl 7:140–155

Crawfurd KJ, Raven JA, Wheeler GL, Baxter EJ, Joint I (2011) The response of *Thalassiosira pseudonana* to long-term exposure to increased CO_2 and decreased pH. PLoS ONE 6:e26695

del R. Gonzalez-Baro M, Pollero RJ (1988) Lipid characterization and distribution among tissues of the fresh-water crustacean *Macrobrachium borellii* during an annual cycle. Comp Biochem Physiol B Biochem Mol Biol 91: 711–715

Dickson AG, Millero FJ (1987) A comparison of the equilibrium-constants for the dissociation of carbonic-acid in seawater media. Deep-Sea Res Part A 34:1733–1743

DOE (US Department of Energy) (1994) Handbook of methods for the analysis of the various parameters of the carbon dioxide system in sea water. Version 2. ORNL/CDIAC-74, http://cdiac.ornl.gov/oceans/DOE-94.pdf

Elser JJ, Sterner RW, Gorokhova E, Fagen WF and others (2000) Biological stoichiometry from genes to ecosystems. Ecol Lett 3:540–550

Feely RA, Sabine CL, Lee K, Berelson W, Kleypas J, Fabry VJ, Millero FJ (2004) Impact of anthropogenic CO_2 on the $CaCO_3$ system in the oceans. Science 305:362–366

Feng Y, Hare CE, Leblanc K, Rose JM and others (2009) Effects of increased pCO_2 and temperature on the North Atlantic spring bloom. I. The phytoplankton community and biogeochemical response. Mar Ecol Prog Ser 388: 13–25

Finkel ZV, Beardall J, Flynn KJ, Quigg A, Rees Ta V, Raven JA (2010) Phytoplankton in a changing world: cell size and elemental stoichiometry. J Plankton Res 32:119–137

Gao KS, Xu JT, Gao G, Li Y and others (2012) Rising CO_2 and increased light exposure synergistically reduce marine primary productivity. Nat Clim Change 2:519–523

Hönisch B, Ridgwell A, Schmidt DN, Thomas E and others (2012) The geological record of ocean acidification. Science 335:1058–1063

Hoppe CJM, Holtz LM, Trimborn S, Rost B (2015) Ocean acidification decreases the light-use efficiency in an Antarctic diatom under dynamic but not constant light. New Phytol 207:159–171

Hutchins DA, Mulholland MR, Fu F (2009) Nutrient cycles and marine microbes in a CO_2-enriched ocean. Oceanography (Wash DC) 22:128–145

IPCC (2007) Climate change 2007: Solomon S, Qin D, Manning M, Chen Z and others (eds) The physical science basis. Contribution of Working Group I to the Fourth Assessment Report of the Intergovernmental Panel on Climate Change. Cambridge University Press, Cambridge

Kainz M, Arts MT, Mazumder A (2004) Essential fatty acids in the planktonic food web and their ecological role for higher trophic levels. Limnol Oceanogr 49:1784–1793

King AL, Sanudo-Wilhelmy SA, Leblanc K, Hutchins DA, Fu FX (2011) CO_2 and vitamin B_{12} interactions determine bioactive trace metal requirements of a subarctic Pacific diatom. ISME J 5:1388–1396

Kump LR, Bralower TJ, Ridgwell A (2009) Ocean acidification in deep time. Oceanography (Wash DC) 22:94–107

Langdon CJ, Waldock MJ (1981) The effect of algal and artificial diets on the growth and fatty-acid composition of *Crassostrea gigas* spat. J Mar Biol Assoc UK 61:431–448

Leu E, Daase M, Schulz KG, Stuhr A, Riebesell U (2013) Effect of ocean acidification on the fatty acid composition of a natural plankton community. Biogeosciences 10: 1143–1153

Martin RE, Quigg A, Podkovyrov V (2008) Marine biodiversification in response to evolving phytoplankton stoichiometry. Palaeogeogr Palaeoclimatol Palaeoecol 258: 277–291

Mayzaud P, Boutoute M, Gasparini S (2013) Differential response of fatty acid composition in the different lipid classes from particulate matter in a high arctic fjord (Kongsfjorden, Svalbard). Mar Chem 151:23–34

Mehrbach C, Culberson CH, Hawley JE, Pytkowicz RM (1973) Measurement of the apparent dissociation constants of carbonic acid in seawater at atmospheric pressure. Limnol Oceanogr 18:897–907

Orr JC, Fabry VJ, Aumont O and others (2005) Anthropogenic ocean acidification over the twenty-first century and its impact on calcifying organisms. Nature 437: 681–686

Parsons TR, Maita Y, Lalli CM (1984) A manual of chemical and biological methods for seawater analysis. Pergamon Press, Oxford

Pierrot D, Lewis E, Wallace DWR (2006) MS Excel program developed for CO_2 system calculations. ORNL/CDIAC-105a. Carbon Dioxide Information Analysis Center, Oak Ridge National Laboratory, US Department of Energy, Oak Ridge, TN, doi:10.3334/CDIAC/otg.CO2SYS_XLS_CDIAC105a

Quigg A, Finkel ZV, Irwin AJ, Rosenthal Y and others (2003) The evolutionary inheritance of elemental stoichiometry in marine phytoplankton. Nature 425:291–294

Reinfelder JR (2012) Carbon dioxide regulation of nitrogen and phosphorus in four species of marine phytoplankton. Mar Ecol Prog Ser 466:57–67

Riebesell U, Zondervan I, Rost B, Tortell PD, Zeebe RE, Morel FMM (2000) Reduced calcification of marine plankton in response to increased atmospheric CO_2. Nature 407:364–367

Riebesell U, Schulz KG, Bellerby RGJ and others (2007) Enhanced biological carbon consumption in a high CO_2

ocean. Nature 450:545–548
Riebesell U, Fabry VJ, Hansson L, Gattuso JP (2010) Guide to best practices for ocean acidification research and data reporting. Publications Office of the European Union, Luxembourg
Riebesell U, Gattuso JP, Thingstad TF, Middelburg JJ (2013) Arctic ocean acidification: pelagic ecosystem and biogeochemical responses during a mesocosm study. Preface. Biogeosciences 10:5619–5626
Roberts K, Granum E, Leegood RC, Raven JA (2007a) C_3 and C_4 pathways of photosynthetic carbon assimilation in marine diatoms are under genetic, not environmental, control. Plant Physiol 145:230–235
Roberts K, Granum E, Leegood RC, Raven JA (2007b) Carbon acquisition by diatoms. Photosynth Res 93:79–88
Rossoll D, Bermudez R, Hauss H, Schulz KG, Riebesell U, Sommer U, Winder M (2012) Ocean acidification-induced food quality deterioration constrains trophic transfer. PLoS ONE 7:e34737
Sabine CL, Feely RA, Gruber N, Key RM and others (2004) The oceanic sink for anthropogenic CO_2. Science 305: 367–371
Sakshaug E, Demers S, Yentsch CM (1987) *Thalassiosira oceanica* and *T. pseudonana*: two different photoadaptational responses. Mar Ecol Prog Ser 41:275–282
Sargent J, Bell G, Mcevoy L, Tocher D, Estevez A (1999) Recent developments in the essential fatty acid nutrition of fish. Aquaculture 177:191–199
Sato N, Tsuzuki M, Kawaguchi A (2003) Glycerolipid synthesis in *Chlorella kessleri* 11 h. II. Effect of the CO_2 concentration during growth. Biochim Biophys Acta 1633: 35–42
Schoo KL, Malzahn AM, Krause E, Boersma M (2013) Increased carbon dioxide availability alters phytoplankton stoichiometry and affects carbon cycling and growth of a marine planktonic herbivore. Mar Biol 160:2145–2155
Shi D, Xu Y, Hopkinson BM, Morel FMM (2010) Effect of ocean acidification on iron availability to marine phytoplankton. Science 327:676–679
Solorzano L, Sharp JH (1980) Determination of total dissolved phosphorus and particulate phosphorus in natural waters. Limnol Oceanogr 25:754–757
Sterner RW, Elser JJ (2002) Ecological stoichiometry: the Biology of elements from molecules to biosphere. Princeton University Press, Princeton, NJ
Tans P (2009) An accounting of the observed increase in oceanic and atmospheric CO_2 and an outlook for the future. Oceanography (Wash DC) 22:26–35
Teoh ML, Chu WL, Marchant H, Phang SM (2004) Influence of culture temperature on the growth, biochemical composition and fatty acid profiles of six Antarctic microalgae. J Appl Phycol 16:421–430
Torstensson A, Hedblom M, Andersson J, Andersson MX, Wulff A (2013) Synergism between elevated pCO_2 and temperature on the Antarctic sea ice diatom *Nitzschia lecointei*. Biogeosciences 10:6391–6401
Tortell PD, Ditullio GR, Sigman DM, Morel FMM (2002) CO_2 effects on taxonomic composition and nutrient utilization in an Equatorial Pacific phytoplankton assemblage. Mar Ecol Prog Ser 236:37–43
Urabe J, Togari J, Elser JJ (2003) Stoichiometric impacts of increased carbon dioxide on a planktonic herbivore. Glob Change Biol 9:818–825
Wacker A, von Elert E (2001) Polyunsaturated fatty acids: evidence for non-substitutable biochemical resources in *Daphnia galeata*. Ecology 82:2507–2520
Wu Y, Gao K, Riebesell U (2010) CO_2-induced seawater acidification affects physiological performance of the marine diatom *Phaeodactylum tricornutum*. Biogeosciences 7:2915–2923
Wu Y, Campbell DA, Irwin AJ, Suggett DJ, Finkel ZV (2014) Ocean acidification enhances the growth rate of larger diatoms. Limnol Oceanogr 59:1027–1034
Wynn-Edwards C, King R, Davidson A, Wright S and others (2014) Species-specific variations in the nutritional quality of southern ocean phytoplankton in response to elevated pCO_2. Water 6:1840–1859
Yang G, Gao KS (2012) Physiological responses of the marine diatom *Thalassiosira pseudonana* to increased pCO_2 and seawater acidity. Mar Environ Res 79:142–151

Editorial responsibility: Katherine Richardson, Copenhagen, Denmark

Submitted: June 2, 2015; Accepted: August 10, 2015
Proofs received from author(s): September 18, 2015